

# K12-biotinylated histone H4 is enriched in telomeric repeats from human lung IMR-90 fibroblasts<sup>☆</sup>

Subhashinee S.K. Wijeratne, Gabriela Camporeale, Janos Zempleni\*

*Department of Nutrition and Health Sciences, University of Nebraska at Lincoln, Lincoln, NE 68583-0806, USA*

Received 2 July 2008; received in revised form 22 December 2008; accepted 8 January 2009

## Abstract

Covalent modifications of histones play a role in regulating telomere attrition and cellular senescence. Biotinylation of lysine (K) residues in histones, mediated by holocarboxylase synthetase (HCS), is a novel diet-dependent mechanism to regulate chromatin structure and gene expression. We have previously shown that biotinylation of K12 in histone H4 (H4K12bio) is a marker for heterochromatin and is enriched in pericentromeric alpha satellite repeats. Here, we hypothesized that H4K12bio is also enriched in telomeres. We used human IMR-90 lung fibroblasts and immortalized IMR-90 cells overexpressing human telomerase (hTERT) in order to examine histone biotinylation in young and senescent cells. Our studies suggest that one out of three histone H4 molecules in telomeres is biotinylated at K12 in hTERT cells. The abundance of H4K12bio in telomeres decreased by 42% during telomere attrition in senescent IMR-90 cells; overexpression of telomerase prevented the loss of H4K12bio. Possible confounders such as decreased expression of HCS and biotin transporters were formally excluded in this study. Collectively, these data suggest that H4K12bio is enriched in telomeric repeats and represents a novel epigenetic mark for cell senescence.  
© 2010 Elsevier Inc. All rights reserved.

**Keywords:** Biotin; Chromatin; Histone; Biotinylation; Human; Telomere

## 1. Introduction

Telomeres, the heterochromatic end caps of linear chromosomes, are composed of thousands of TTAGGG repeats in human chromatin and bind proteins such as TRF1 (telomeric repeat binding factor 1), TRF2 and tankyrase [1–3]. Telomeres play an important role in chromosome stability by preventing the loss or mutations of genes and the fusion of chromosomes [1,4,5]. Due to the inability of DNA polymerases to replicate the end of chromosomes, telomere length is shortened by approximately 50–150 bp with each cell division [6]. Division ceases when telomeres reach a critical threshold length in senescent cells [6–8]. In germline cells, immortalized cell lines and cancer cells, telomere shortening is prevented by telomerase, which is composed of two major components, the telomerase reverse transcriptase and telomerase RNA template. Telomerase helps to maintain telomere length by adding TTAGGG repeats to the chromosome ends during replication [9–13].

Chromatin structure and gene expression are regulated by covalent modifications of histones H1, H2A, H2B, H3 and H4 [14,15]. DNA and histones form the nucleosomal core particles, which consist of 146 bp of DNA wrapped around an octamer of core histones (one H3–H3–H4–H4 tetramer and two H2A–H2B dimers) [16]. Histone H1 binds to the DNA in between two nucleosomal core particles, completing the nucleosomal assembly [16]. The amino-terminal tails of histones that protrude from the nucleosomal surface are subjected to various covalent modifications [17,18]. Acetylation, phosphorylation and methylation of histone tails play a major role in regulating telomere attrition by controlling telomerase activity [19–21].

Recently, it was shown that biotinylation of lysine (K) residues in histones, a novel diet-dependent histone modification, plays a role in gene regulation [22–24]. Biotinylation is mediated by holocarboxylase synthetase (HCS) [23,25]. Human histone biotinylation sites include K9, K13, K125, K127 and K129 in histone H2A [26]; K4, K9, K18 and perhaps K23 in histone H3 [27,28]; and K8 and K12 in histone H4 [29].

We have shown that K12-biotinylated histone H4 (H4K12bio) is enriched in repeat regions such as pericentromeric alpha satellite repeats and retrotransposons and also participates in gene repression [24,30]. Here, we tested the hypothesis that H4K12bio is a general marker for repeat regions and, therefore, is enriched in telomeric repeats. We propose that decreased abundance of H4K12bio is an epigenetic mark for cell senescence.

<sup>☆</sup> We would like to acknowledge the contribution of the University of Nebraska Agricultural Research Division, supported in part by funds provided through the Hatch Act. Additional support was provided by NIH Grants DK063945, DK077816 and ES015206; by USDA CSREES Grant 2006-35200-17138; and by NSF EPSCoR Grant EPS-0701892.

\* Corresponding author. Tel.: +1 402 472 3270; fax: +1 402 472 1587.  
E-mail address: [jzempleni2@unl.edu](mailto:jzempleni2@unl.edu) (J. Zempleni).

In this study, we used primary human IMR-90 lung fibroblasts as a model to investigate histone biotinylation in aging cells. IMR-90 cells were chosen because they undergo telomere attrition and enter a state of irreversible growth arrest, designated cellular senescence, after about 50–55 population doublings (PDs). IMR-90 cells overexpressing human telomerase reverse transcriptase (hTERT cells) do not undergo senescence [31] and were used as immortal controls. Our goals were to determine (a) whether H4K12bio is enriched in telomeric repeats in human cells, (b) whether the abundance of H4K12bio decreases with aging and (c) whether overexpression of telomerase prevents loss of H4K12bio.

## 2. Methods and materials

### 2.1. Cell culture

Human lung fibroblast IMR-90 cells were purchased from American Type Culture Collection (Manassas, VA). These cells were passaged two to three times per week and replated at 60,000 to 80,000 cells in T75 cell culture flasks with 15 ml medium. IMR-90 cells were harvested at timed intervals. Young cells at PD 35 were used as baseline. IMR-90 cells were considered to be senescent when they did not need to be passaged for 2 weeks, and at this stage, they were at a PD of 50–55. hTERT cells were kindly provided by Dr. Judith Campisi (Lawrence Berkeley National Laboratory, California) at PD 55. hTERT cells at PD 60 were used as baseline and harvested at 5 or 10 additional PDs. Cells were cultured in Minimum Essential Medium supplemented with 10% (v/v) fetal bovine serum, 0.1% nonessential amino acids, 100,000 U/L penicillin and 100 mg/L streptomycin.

### 2.2. $\beta$ -Galactosidase ( $\beta$ -gal) staining

Senescent cells are known to express  $\beta$ -gal, which produces a blue color in the  $\beta$ -gal assay; the  $\beta$ -gal assay was performed as described previously [32].

### 2.3. Telomerase activity

Telomerase activity was detected by telomerase repeat amplification protocol (TRAP) assay [33] with slight modifications. In this assay, telomerase from cell extracts ligates synthetic TTAGGG repeats to the 3' end of the telomerase substrate oligonucleotide "TS" (5'-AATCCGTCGACGAGATT-3'). The extended product is then amplified by PCR using TS and the reverse primer CX (5'-CCTTACCCTTACCCTTACCCTAA-3'), which generates a ladder of PCR products with size increasing in six-base increments starting at 50 nucleotides. Cell lysate [33] was incubated on ice for 30 min and centrifuged at 12,000 $\times$ g for 20 min at 4°C. The protein concentrations in lysates were adjusted to 1 g/L by dilution with lysis buffer; 2  $\mu$ l of lysate was used in TRAP reaction as follows. PCR amplification of telomerase extension products was performed in 50- $\mu$ l TRAP reaction mixes containing 20 mM Tris-HCl (pH 8.3), 1.5 mM MgCl<sub>2</sub>, 68 mM KCl, 0.005% Tween 20, 1 mM EGTA, 50  $\mu$ M dNTP, TS and CX primers at 1.8 mg/L and 2 U of *Taq* polymerase. Samples were denatured for 2 min at 94°C, followed by 30 cycles of PCR amplification at 94°C for 10 s, 50°C for 25 s and 72°C for 30 s in a thermal cycler. Samples were analyzed using 10% TBE gels (Invitrogen, Carlsbad, CA) with 0.5 mg/L ethidium bromide staining.

### 2.4. Telomere length assay using real-time PCR

Relative telomere lengths were determined as described previously [34] with slight modifications using the iCycler iQ multicolor real-time detection system (Bio-Rad, Palo Alto, CA). The relative telomere lengths were determined as the factor by which a genomic DNA sample differs from a reference sample in its ratio of telomere (*T*) repeat copy number to a single (*S*) copy gene number. The cycle threshold (*Ct*) values generated were used to calculate *T/S* values for each sample:  $T/S = 2^{-\Delta Ct}$  (where  $\Delta Ct = Ct_{\text{singlecopygene}} - Ct_{\text{telomere}}$ ). Long telomeres produce low *Ct* values because more PCR product is generated due to many PCR initiation sites; this results in higher *T/S* ratios. Genomic DNA was extracted from IMR-90 (PDs 35 and 45) and hTERT cells (PD *n* and PD *n*+10). Standard curves were generated for telomeres and the single-copy gene; DNA concentrations in standards ranged from 10 to 100 ng/reaction. Triplicate PCR reactions were carried out in a 25- $\mu$ l total reaction mix containing Absolute QPCR SYBR Green fluorescein mix (ABgene, Rochester, NY). Primers for telomeres (T1a and T1b) and the single-copy gene 36B4 (acidic ribosomal phosphoprotein PO) were added to obtain final concentrations of 0.2 and 0.3  $\mu$ M, respectively [34].

### 2.5. Chromatin immunoprecipitation (ChIP) assay

IMR-90 and hTERT cells were used to quantify the relative enrichment of proteins in telomeric repeats. ChIP assays were conducted as described previously [24]. The following antibodies were used for ChIPs: polyclonal antisera against H4K12bio [29] and antibodies against telomere protein TRF2 and the C-terminus in histone H3

(Abcam, Cambridge, MA). Efficiency of anti-H4K12bio in ChIP assays was tested by comparing nuclear extracts from ChIP assays before and after treatment with anti-H4K12bio; in these assays, supernatants from before and after immunoprecipitation were probed with anti-H4K12bio using Western blot analysis [29]. Chromatin immunoprecipitated with the preimmune serum of H4K12bio served as the negative control. Each immunoprecipitation was repeated three times, using 47 million cells per precipitation. Cross-links were reversed, and DNA was recovered for ligation-mediated PCR (LMPCR). For total DNA samples (denoted input DNA), aliquots corresponding to one sixth of the lysate volume used for immunoprecipitation were processed along with the rest of immunoprecipitated samples during the cross-link reversal step. DNA was amplified by LMPCR as described previously [35,36] with the following modifications. An asymmetric double-stranded T7 linker composed of a 25-mer (5'-GGCTAATACGACTCATAGGGAG-3') annealed to a 13-mer (5'-CTCCCTATAGTGA-3') was prepared by dissolving 670 pmol of each oligonucleotide in 100  $\mu$ l of water, heating at 95°C for 5 min and cooling to room temperature. Blunt-end DNA was produced by mixing 25 ng of input or antibody-precipitated DNA and 5 U T4 DNA polymerase (Invitrogen). Blunt-end DNA was purified by using QIAprep Spin Miniprep Kit (Qiagen, Inc., Valencia, CA) and resuspended in 20  $\mu$ l of 10 mM Tris-Cl, pH 8.5. DNA was ligated to the T7 linker by incubating with 5 U T4 DNA Ligase (Ambion, Austin, TX) at 16°C overnight. Ligation products were purified by eluting with 20  $\mu$ l of 10 mM Tris-HCl, pH 8.5, using QIAprep Spin Miniprep Kits. Ligation products were PCR amplified twice. First, 18- $\mu$ l ligation products were amplified for 20 cycles by using 50 pmol 25-mer linker primer and 5 U *Taq* DNA polymerase (New England Biolabs, Ipswich, MA) as follows: 94°C for 30 s, 55°C for 30 s and 72°C for 1 min 15 s, followed by a final extension at 72°C for 4 min. Ligation products were purified by eluting with 20  $\mu$ l of 10 mM Tris-HCl, pH 8.5, using Miniprep Kits, and subjected to another 20 cycles of PCR under the same conditions as above. Ligation products were purified by eluting with 20  $\mu$ l of ddH<sub>2</sub>O using Spin Miniprep Kits.

Equal amounts of input and immunoprecipitated DNA were dot blotted onto a nylon membrane and fixed with UV cross-linking. Membranes were dried and hybridized using <sup>32</sup>P-labeled (CCCTAA)<sub>4</sub> as a probe for telomeric repeats. Intensities of dots were determined using Image J 1.38x software [37]. Dot blot analysis data (relative intensities of dots) were obtained for three independent blots. Input DNA represents the total telomeric DNA in cell extracts. The amount of telomeric DNA immunoprecipitated in each ChIP was calculated based on the signal relative to the corresponding total telomeric (input) DNA. ChIP data are reported as ratios of immunoprecipitated DNA to an equal amount of input DNA.

Co-immunoprecipitation experiments were conducted to confirm physical interaction between TRF2 and H4K12bio. In these experiments, nuclear extracts from ChIP assays were precipitated with anti-H4K12bio, followed by Western blot analysis with anti-TRF2 [29,38].

### 2.6. Abundance of biotinylated histones

Nuclear histones were extracted from IMR-90 and hTERT cells using 1 M HCl [22]. Histones were resolved on 18% Tris-glycine gels (Invitrogen). Transblots were probed with streptavidin peroxidase [22] and the following primary antibodies: rabbit anti-human H4K12bio [29], rabbit anti-human H3K9bio and rabbit anti-human H3K18bio [27]. Rabbit anti-human H4K20me3 (Abcam) is a known marker for aging [39] and was used as a control. Antibody and avidin blots were quantified using chemiluminescence and gel densitometry [40]. Equal loading of lanes and sample integrity was confirmed by using bicinchoninic assay (Pierce, Rockford, IL), densitometric quantitation of gels stained with Coomassie blue and Western blot analysis using an antibody to the C-terminus in histone H3 (Santa Cruz Biotechnology, Santa Cruz, CA).

### 2.7. Abundance of HCS protein and mRNA and biotin-dependent carboxylases

Abundance of HCS in whole-cell homogenates was quantified by Western blot analysis as described previously [41]. Histone H3 (Santa Cruz Biotechnology) was used as loading control [41]. Abundance of mRNA coding for HCS was quantified as described previously [41]. HCS is also responsible for catalyzing the attachment of biotin to acetyl-CoA carboxylase 1 and 2, pyruvate carboxylase (PC), propionyl-CoA carboxylase (PCC) and 3-methylcrotonyl-CoA carboxylase (MCC) [41]. Abundance of these holocarboxylases was quantified by streptavidin blotting as described previously [42]. Equal loading of protein was confirmed by gel densitometry after probing with anti-human histone H3.

### 2.8. Biotin transporter expression

The abundance of biotin transporter (SMVT) protein and mRNA was quantified as described previously [41]. Rates of biotin transport into IMR-90 cells were determined using [<sup>3</sup>H]biotin at a physiological concentration of 475 pmol/L as described previously [43].

### 2.9. Statistics

Homogeneity of variances among groups was confirmed using Bartlett's test [44]. Significance of differences among groups was tested by one-way ANOVA. Fisher's

protected least significant difference procedure was used for post hoc testing [44]. StatView 5.0.1 (SAS Institute, Cary, NC) was used to perform all calculations. Differences were considered significant if  $P \leq 0.05$ . Data are expressed as mean  $\pm$  S.D.

### 3. Results

#### 3.1. Validation of cell models

IMR-90 cell cultures were harvested at PDs 35, 40 and 45. hTERT cells were received at PD 55 and harvested at PDs 60, 65 and 70, which are referred to as  $n$ ,  $n+5$  and  $n+10$  in the text. Telomere length, telomerase activity and  $\beta$ -gal activity were measured to validate our cell models.

Relative telomere length was quantified as the ratio of telomere ( $T$ ) repeat copy number to a single ( $S$ ) copy gene number ( $T/S$  ratio) in a genomic DNA sample. The  $T/S$  ratio is directly proportional to the average telomere length [34,45]. The  $T/S$  ratios for IMR-90 cells at PDs 35, 40 and 45 were  $1.0 \pm 0.1$ ,  $0.9 \pm 0.01$  and  $0.7 \pm 0.03$ , respectively, consistent with telomere attrition in aging cells. The  $T/S$  ratios of hTERT cells (control) were  $1.0 \pm 0.1$  and  $1.1 \pm 0.1$  at PDs  $n$  and  $n+10$ , respectively, indicating no change in telomere length. Telomerase activity was detectable in hTERT cells (positive control) but absent in both IMR-90 cells and heat-treated hTERT cells (negative control, Fig. 1).  $\beta$ -Gal is a known marker for cell senescence [32];  $\beta$ -gal activity was detected in IMR-90 (PD 45) but not in hTERT ( $n+10$ ) cells (Fig. 2). IMR-90 cells ceased to proliferate at about PD 55, whereas hTERT cells continued to proliferate during the entire observation period (data not shown). These results confirm that IMR-90 cells undergo senescence and show decreasing telomere lengths with aging, whereas telomerase-expressing hTERT cells escape senescence and maintain their telomeres during cell division.

#### 3.2. Histone biotinylation in telomeric repeats

Previous studies suggested that H4K12bio is enriched in repeat regions such as pericentromeric alpha satellite repeats and retrotransposons [24,30]. Here, we used ChIP assays in combination with dot blotting to demonstrate that H4K12bio is also enriched in telomeric repeats.

Chromatin from hTERT and IMR-90 cells was precipitated with antibodies to H4K12bio, the C-terminus in histone H3 and TRF2; spotted onto a nylon membrane; and probed with a telomere-

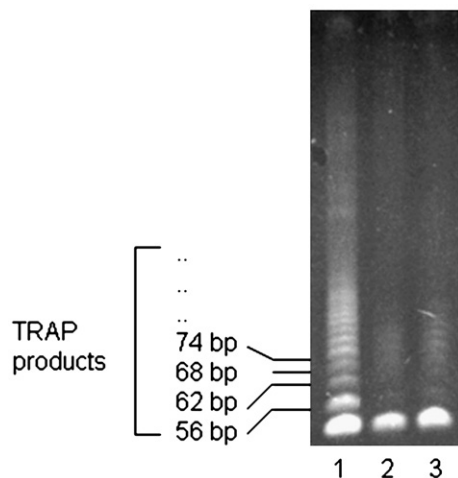


Fig. 1. Telomerase activity is present in cell extracts from hTERT-immortalized fibroblasts (lane 1) but not in heat-treated extract from hTERT-immortalized fibroblasts (lane 2) and nontreated IMR-90 fibroblasts (lane 3).

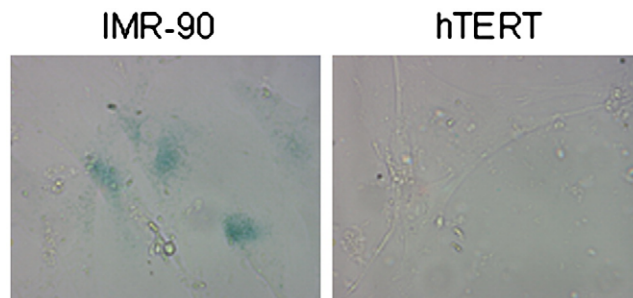


Fig. 2.  $\beta$ -Gal activity is detectable in IMR-90 fibroblasts (PD 45) but not in hTERT-immortalized fibroblasts (PD  $n+10$ ).

specific oligonucleotide (Fig. 3). Relative enrichment of telomeric repeats in each ChIP was quantified as the signal intensity relative to the corresponding telomeric signal in total genomic DNA (input DNA). In this assay, input DNA represents the total amount of telomeric repeats, whereas precipitation with anti-H4K12bio, anti-histone H3 and anti-TRF2 is a marker for the relative enrichment of these proteins in telomeric repeats. All three proteins were associated with telomeric repeats (Fig. 3A). Dot blot analyses of hTERT ChIP suggested that  $31 \pm 4\%$  of the histone H4 in telomeric repeats is biotinylated at K12 ( $n=3$ ). This calculation was based on the fact that equal amounts of H3 and H4 exist in nucleosomes [16,46] and that the relative enrichments of telomeric repeats in pull-down DNA with anti-H4K12bio, anti-histone H3 and anti-TRF2 were 0.3, 1.0 and 1.5, respectively, in hTERT cells. Note that the C-terminus in histone H3 is not known to be covalently modified and that ChIP with anti-H3 is a well-established marker for quantitation of nucleosomal abundance [47–49]. The relative enrichments depended on the PD (0.8, 1.0 and 1.1 at PD 35 vs. 0.6, 1.0 and 1.1 at PD 45) in IMR-90 cells (Fig. 3B). Furthermore, ChIP data from IMR-90 showed that the relative enrichment of telomeric repeats in total telomeric DNA (input DNA) was reduced by 23%, whereas the pull-down DNA with anti-H4K12bio, anti-histone H3 and anti-TRF2 decreased by 42%, 25% and 24%, respectively, at PD 45 compared to those of PD 35, confirming the association of H4K12bio with telomeres. Co-immunoprecipitation experiments confirmed that TRF2 physically interacts with H4K12bio, consistent with enrichment of H4K12bio in telomeres (Fig. 3C). Note that the abundance of H4K12bio in telomeres is an estimate that should be interpreted carefully, as it somewhat depends on the affinity and quality of antibodies used in ChIP assays. Importantly, our studies suggest that our anti-H4K12bio antibody in combination with our protocol for ChIP assays produced a near-complete precipitation of H4K12bio in nuclear extracts (Fig. 4); incubation with preimmune serum did not produce a meaningful depletion of H4K12bio in nuclear extracts (negative control).

#### 3.3. Histone biotinylation in aging cells

Based on our observation that H4K12bio is enriched in telomeres, we expected to see an age-dependent decrease in biotinylation of histones in bulk histone extracts from IMR-90 nuclei but not from hTERT cell nuclei. When IMR-90 nuclear histones were probed with streptavidin, which is a probe for biotin regardless of the biotinylation sites in histones, the abundance of biotinylated histones was  $20 \pm 4.3\%$  lower in PD 45 cells compared with PD 35 cells (Fig. 5A) as judged by gel densitometry. Next, we looked at distinct biotinylation sites. The abundance of H4K12bio significantly decreased by  $85 \pm 8.4\%$  at PD 45 compared to PD 35 in IMR-90 cells (Fig. 5B). In contrast,

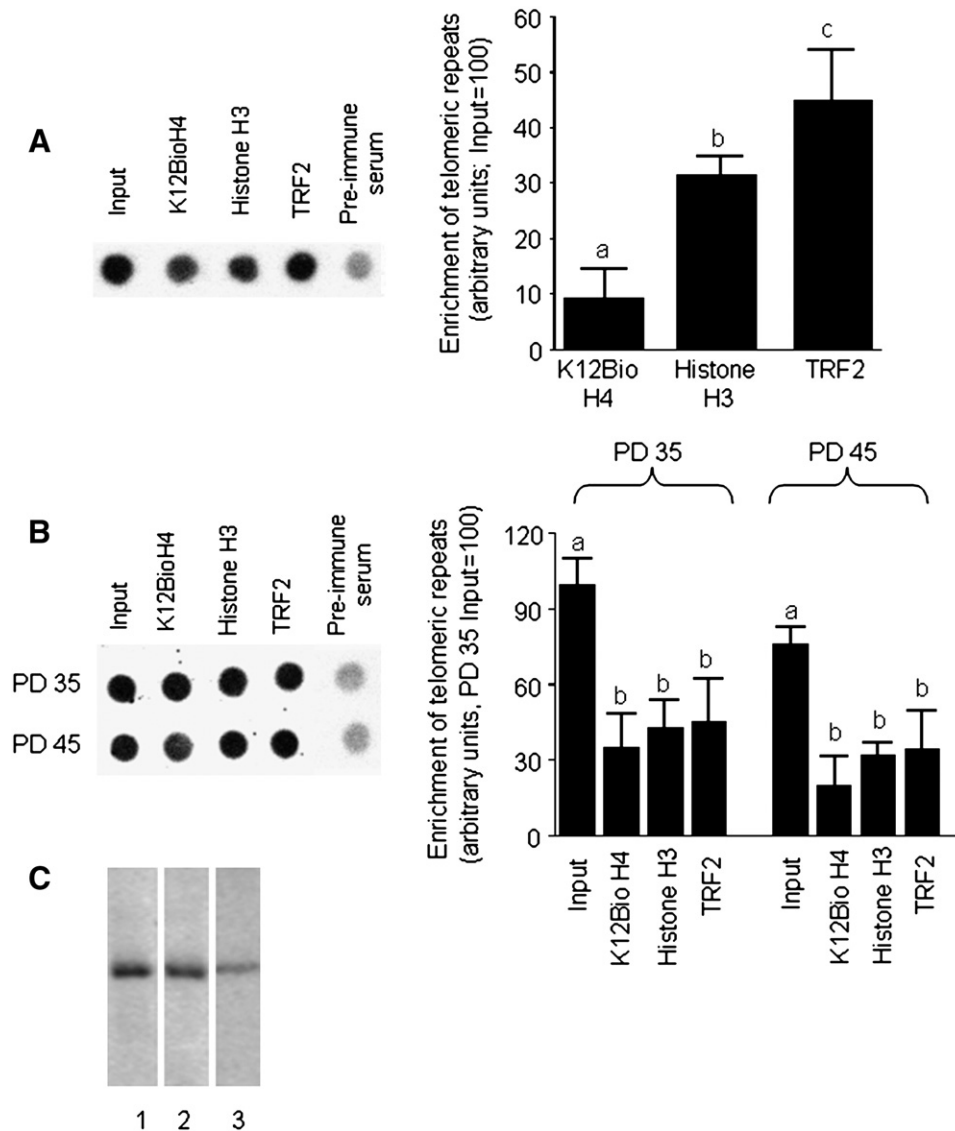


Fig. 3. H4K12bio is associated with telomeric repeats. Chromatin was immunoprecipitated from hTERT and IMR-90 cells using antibodies to H4K12bio, the C-terminus in histone H3, TRF2 and preimmune serum (negative control); DNA was amplified by LMP-PCR, dot blotted onto a nylon membrane and probed with a  $^{32}\text{P}$ -labeled telomeric probe. (A) Left panel: dot blots of input DNA and precipitated DNA from hTERT cells. Spots from the same blot were electronically rearranged to facilitate comparisons. Right panel: the enrichment of telomeric repeats in immunoprecipitated DNA relative to total telomeric DNA (input DNA) in arbitrary units. Bars represent means  $\pm$  S.D.,  $n=3$ . (B) Left panel: dot blots of input DNA and precipitated DNA from IMR-90 cells. Right panel: the enrichment of telomeric repeats in immunoprecipitated DNA at PDs 35 and 45 relative to their corresponding input DNA in IMR-90 cells. Bars represent means  $\pm$  S.D.,  $n=3$ . <sup>a,b</sup>Bars not sharing the same letter are significantly different for the same PD ( $P \leq 0.05$ ). (C) H4K12bio colocalizes with TRF2 in chromatin. Chromatin in nuclear extracts was immunoprecipitated with anti-TRF2 (lane 1), anti-H4K12bio (lane 2) or preimmune serum (lane 3), and TRF2 in precipitates was probed using Western blot analysis and anti-TRF2.

biotinylation of K9 and K18 in histone H3 showed no change (Fig. 5C and D). The known aging marker K20 trimethylated in histone H4 (H4K20me3) [39] increased with aging in IMR-90 cells (positive control, Fig. 5E). There was no change in hTERT cells if histones were probed with antibodies to H4K12bio, H3K9bio, H3K18bio and H4K20me3. Staining with Coomassie blue and probing with anti-histone H3 were used to confirm equal loading of histones from within each group (Fig. 5F and G).

#### 3.4. Abundance of HCS, SMVT and carboxylases

Theoretically, the expression of HCS [23,25] and the biotin transporter SMVT [50] might affect histone biotinylation. Therefore, we investigated the expression of these proteins in IMR-90 and hTERT cells. The expression of HCS (as judged by mRNA and protein

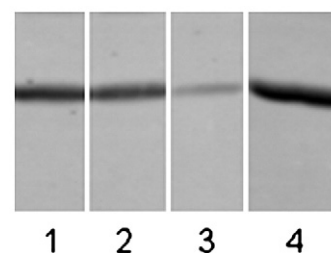


Fig. 4. Immunoprecipitation with anti-H4K12bio precipitates nearly the entire H4K12bio in nuclear extracts. Nuclear extracts from hTERT cells were treated with anti-H4bioK12 or preimmune serum (negative control) in ChIP assays. Nuclear extracts before precipitation and bulk extracts of nuclear histones served as controls. Lane 1, nuclear extract before immunoprecipitation; lane 2, nuclear extract after immunoprecipitation with preimmune serum; lane 3, nuclear extract after immunoprecipitation with anti-H4K12bio; lane 4, bulk histone extracts from hTERT cells probed with anti-H4K12bio.

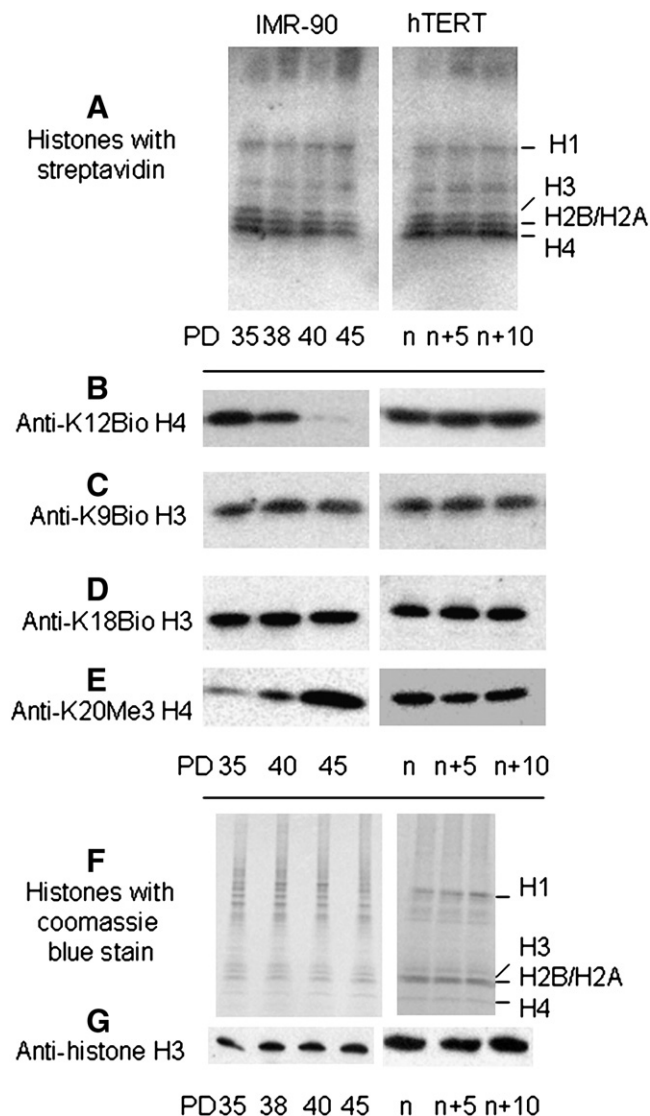


Fig. 5. H4K12bio decreases in senescent IMR-90 fibroblasts but not in hTERT-immortalized fibroblasts. Bulk histones were extracted from cells at different PDs and biotin was probed as follows. (A) Streptavidin, (B) anti-H4K12bio, (C) anti-H3K9bio, (D) anti-H3K18bio and (E) anti-H4K20me3. Equal loading for each cell type was confirmed by (F) staining with Coomassie blue and (G) probing with anti-histone H3.

abundance) and SMVT (abundance of mRNA and protein and biotin transport rates) did not change in hTERT cells during the observation period (data not shown). Similarly, the expression of HCS did not change in IMR-90 cells (data not shown). In contrast, the abundance of SMVT mRNA and protein decreased by  $25 \pm 2.1\%$  and  $65 \pm 5.2\%$ , respectively, in PD 45 compared to PD 35 in IMR-90 cells (Fig. 6A and B). The decreased expression of SMVT in aging IMR-90 cells was paralleled by a decrease in biotin transport rates. Biotin transport rates decreased from  $49 \pm 1.2$  to  $18 \pm 1.1$  amol/( $\mu\text{g protein} \times 30 \text{ min}$ ) at PD 35 and PD 45, respectively, in IMR-90 cells (Fig. 6C).

Holocarboxylases are a well-established marker of biotin status [42,51]. Therefore, we quantified holocarboxylases to determine whether the decreased expression of biotin transporters in aging IMR-90 cells decreased the intracellular levels of biotin. The abundance of biotinylated PC, PCC and MCC did not change in hTERT cells (PD  $n+10$  vs. PD  $n$ ). In contrast, biotinylation of PC

decreased by  $40 \pm 4.2\%$  at PD 45 compared with PD 35 in IMR-90 cells (Fig. 7A,  $P < .05$ , PD 45 vs. PD 35;  $n=3$ ). Biotinylation of PCC and MCC decreased to a similar extent in aging IMR-90 cells. Equal loading of carboxylases was confirmed by probing with anti-histone H3 (Fig. 7B).

#### 4. Discussion

Here, we report a novel epigenetic mark for telomeric repeats in humans, H4K12bio. Our studies suggest that about one third of the histones H4 in telomeres are biotinylated in position K12. Consistent with this observation, telomere attrition in aging cells was associated with a loss of H4K12bio. This loss of H4K12bio was prevented by overexpression of hTERT. Aging had no effect on the biotinylation of histones other than H4. These observations are

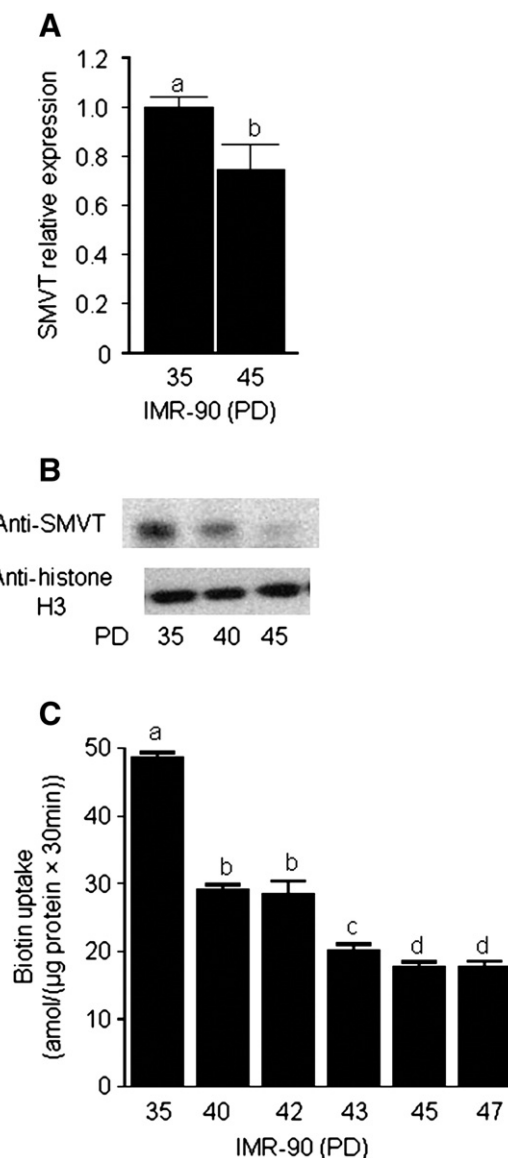


Fig. 6. Abundance of SMVT and biotin transport rates decrease in senescent IMR-90 cells. (A) Abundance of SMVT mRNA was quantified using RT-PCR. (B) Whole-cell lysates from cells at different PDs were probed with anti-SMVT. (C) Cells at different PDs were harvested and biotin transport rates were measured using [ $^3\text{H}$ ]biotin at a concentration of 475 pmol/L. Bars represent mean  $\pm$  S.D.,  $n=3$ . <sup>a,b,c,d</sup> Bars not sharing the same letter are significantly different ( $P \leq .05$ ).

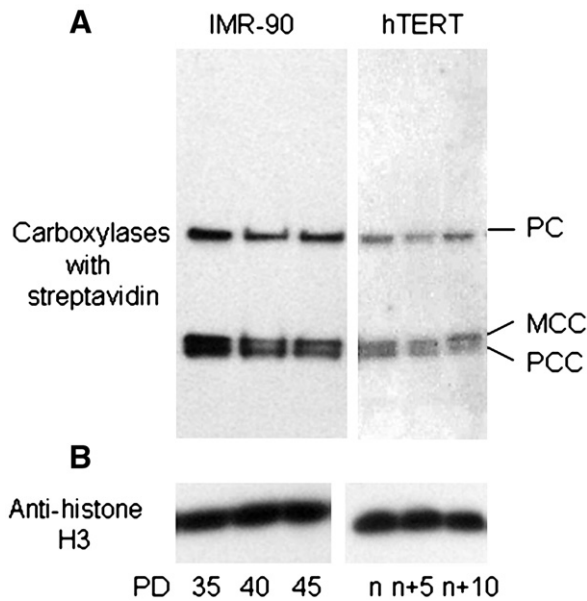


Fig. 7. Abundance of holocarboxylases decreases in senescent IMR-90 cells but not in hTERT cells. (A) Whole-cell lysates from cells at different PDs were extracted and probed with streptavidin as a probe for biotin in PC, MCC and PCC. (B) Equal loading for each cell type was confirmed by probing with anti-histone H3.

consistent with previous studies in our laboratory in which we demonstrated that H4K12bio is a mark for repeat regions and repressed genes [24,41].

In this study, we have formally excluded a number of potential confounders that might affect biotinylation of histones. First, we have shown that the expression of HCS does not depend on aging. Therefore, the low abundance of H4K12bio in aging cells is not caused by a decrease in the levels of this essential histone biotinylation enzyme [25]. In previous studies, we have demonstrated that another putative histone biotinylation enzyme, biotinidase, is less important than HCS for histone biotinylation [23]. Second, we have shown that the cellular availability of biotin in aging IMR-90 cells was sufficient to maintain biotinylation of carboxylases despite a decreased expression of the determined biotin transporter SMVT. We demonstrated that biotin transport rates decreased by about 60% in aging cells compared with young cells but that effects on biotinylation of carboxylases, PC, PCC and MCC, were moderate (<40%) compared with decreased abundance of H4K12bio (>85%) in these cells. Previous studies in human cell lines suggest that biotinylation of carboxylases is an early and sensitive marker for cellular biotin levels [42,52,53].

Theoretically, the difference between the depletion of holocarboxylases and H4K12bio could have been caused by distinct turnover rates of these proteins. The half-lives of carboxylases are only a few days [54–58], whereas half-lives of histones may extend to several weeks depending on the type of tissue and class of histone investigated [59,60]. Therefore, it is unlikely that the decrease in H4K12bio seen in this study was caused by a rapid turnover of this protein, although we cannot formally exclude this possibility. We propose that telomere attrition is responsible for the depletion of H4K12bio in aging cells.

In this study, the abundance of H3K9bio and H3K18bio in bulk histones was not affected by aging. Functions of K9- and K18-biotinylated histone H3 are unknown and are currently being investigated in our laboratory along with other known histone biotinylation marks [26–29]. Preliminary studies suggest that some of these biotinylation marks are enriched in transposable elements, such as long terminal repeats in humans and mice [30].

The structural function of H4K12bio in telomeres is unknown, but it appears to be related to gene repression and heterochromatin formation [24]. In addition, please note that telomeres bind to the nuclear envelope, mediated by proteins such as membrane telomere binding protein, SUN1 and SUN2 [61–63]. HCS also localizes primarily to the nuclear lamina [25], but any mechanistic links between HCS, nuclear compartmentalization and telomeres are unknown. We are now in the process of identifying proteins that interact with HCS, and our ongoing studies tentatively revealed a number of proteins that may play critical roles in chromatin biology.

## References

- [1] Greider CW. Telomeres, telomerase and senescence. *Bioessays* 1990;12:363–9.
- [2] Smith S, Giriat I, Schmitt A, de Lange T. Tankyrase, a poly(ADP-ribose) polymerase at human telomeres. *Science* 1998;282:1484–7.
- [3] Broccoli D, Smogorzewska A, Chong L, de Lange T. Human telomeres contain two distinct Myb-related proteins, TRF1 and TRF2. *Nat Genet* 1997;17:231–5.
- [4] Greider CW. Telomerase is processive. *Mol Cell Biol* 1991;11:4572–80.
- [5] Blackburn EH, Greider CW. *Telomeres*. Plainview (NY): Cold Spring Harbor Laboratory Press; 1995.
- [6] Kipling D. Telomeres, replicative senescence and human ageing. *Maturitas* 2001;38:25–38.
- [7] Chiu CP, Harley CB. Replicative senescence and cell immortality: the role of telomeres and telomerase. *Proc Soc Exp Biol Med* 1997;214:99–106.
- [8] Karlseder J, Smogorzewska A, de Lange T. Senescence induced by altered telomere state, not telomere loss. *Science* 2002;295:2446–9.
- [9] Greider CW, Blackburn EH. Identification of a specific telomere terminal transferase activity in Tetrahymena extracts. *Cell* 1985;43:405–13.
- [10] Greider CW, Blackburn EH. A telomeric sequence in the RNA of Tetrahymena telomerase required for telomere repeat synthesis. *Nature* 1989;337:331–7.
- [11] Blackburn EH, Greider CW, Henderson E, Lee MS, Shampay J, Shippen-Lentz D. Recognition and elongation of telomeres by telomerase. *Genome* 1989;31:553–60.
- [12] Blackburn EH. Telomerases. *Annu Rev Biochem* 1992;61:113–29.
- [13] Nugent CI, Lundblad V. The telomerase reverse transcriptase: components and regulation. *Genes Dev* 1998;12:1073–85.
- [14] Grewal SI, Moazed D. Heterochromatin and epigenetic control of gene expression. *Science* 2003;301:798–802.
- [15] Khan AU, Krishnamurthy S. Histone modifications as key regulators of transcription. *Front Biosci* 2005;10:866–72.
- [16] Wolffe A. *Chromatin*. San Diego (CA): Academic Press; 1998.
- [17] Jenwein T, Allis CD. Translating the histone code. *Science* 2001;293:1074–80.
- [18] Fischle W, Wang Y, Allis CD. Histone and chromatin cross-talk. *Curr Opin Cell Biol* 2003;15:172–83.
- [19] Cong YS, Bacchetti S. Histone deacetylation is involved in the transcriptional repression of hTERT in normal human cells. *J Biol Chem* 2000;275:35665–8.
- [20] Devereux TR, Horikawa I, Anna CH, Annab LA, Afshari CA, Barrett JC. DNA methylation analysis of the promoter region of the human telomerase reverse transcriptase (hTERT) gene. *Cancer Res* 1999;59:6087–90.
- [21] Ge Z, Liu C, Bjorkholm M, Gruber A, Xu D. Mitogen-activated protein kinase cascade-mediated histone H3 phosphorylation is critical for telomerase reverse transcriptase expression/telomerase activation induced by proliferation. *Mol Cell Biol* 2006;26:230–7.
- [22] Stanley JS, Griffin JB, Zemleni J. Biotinylation of histones in human cells: effects of cell proliferation. *Eur J Biochem* 2001;268:5424–9.
- [23] Camporeale G, Giordano E, Rendina R, Zemleni J, Eissenberg JC. *Drosophila* holocarboxylase synthetase is a chromosomal protein required for normal histone biotinylation, gene transcription patterns, lifespan and heat tolerance. *J Nutr* 2006;136:2735–42.
- [24] Camporeale G, Oommen AM, Griffin JB, Sarath G, Zemleni J. K12-biotinylated histone H4 marks heterochromatin in human lymphoblastoma cells. *J Nutr Biochem* 2007;18:760–8.
- [25] Narang MA, Dumas R, Ayer LM, Gravel RA. Reduced histone biotinylation in multiple carboxylase deficiency patients: a nuclear role for holocarboxylase synthetase. *Hum Mol Genet* 2004;13:15–23.
- [26] Chew YC, Camporeale G, Kothapalli N, Sarath G, Zemleni J. Lysine residues in N- and C-terminal regions of human histone H2A are targets for biotinylation by biotinidase. *J Nutr Biochem* 2006;17:225–33.
- [27] Kobza K, Camporeale G, Rueckert B, Kueh A, Griffin JB, Sarath G, Zemleni J. K4, K9, and K18 in human histone H3 are targets for biotinylation by biotinidase. *FEBS J* 2005;272:4249–59.
- [28] Kobza K, Sarath G, Zemleni J. Prokaryotic BirA ligase biotinylates K4, K9, K18 and K23 in histone H3. *BMB Rep* 2008;41:310–5.
- [29] Camporeale G, Shubert EE, Sarath G, Cerny R, Zemleni J. K8 and K12 are biotinylated in human histone H4. *Eur J Biochem* 2004;271:2257–63.
- [30] Chew YC, West JT, Kratzer SJ, Ilvarsson AM, Eissenberg JC, Dave BJ, Klinkebiel D, Christman JK, Zemleni J. Biotinylation of histones represses transposable elements in human and mouse cells and cell lines, and in *Drosophila melanogaster*. *J Nutr* 2008;138:2316–22.

- [31] Rubio MA, Kim SH, Campisi J. Reversible manipulation of telomerase expression and telomere length. Implications for the ionizing radiation response and replicative senescence of human cells. *J Biol Chem* 2002;277:28609–17.
- [32] Dimri GP, Lee X, Basile G, Acosta M, Scott G, Roskelley C, Medrano EE, Linskens M, Rubelj I, Pereira-Smith O, et al. A biomarker that identifies senescent human cells in culture and in aging skin in vivo. *Proc Natl Acad Sci USA* 1995;92:9363–7.
- [33] Kim NW, Piatyszek MA, Prowse KR, Harley CB, West MD, Ho PL, Coviello GM, Wright WE, Weinrich SL, Shay JW. Specific association of human telomerase activity with immortal cells and cancer. *Science* 1994;266:2011–5.
- [34] Gil ME, Coetzer TL. Real-time quantitative PCR of telomere length. *Mol Biotechnol* 2004;27:169–72.
- [35] Kang SH, Vieira K, Bungert J. Combining chromatin immunoprecipitation and DNA footprinting: a novel method to analyze protein–DNA interactions in vivo. *Nucleic Acids Res* 2002;30:e44.
- [36] Hornstra IK, Yang TP. In vivo footprinting and genomic sequencing by ligation-mediated PCR. *Anal Biochem* 1993;213:179–93.
- [37] Rasband W. ImageJ 1.39t software. (<http://rsb.info.nih.gov/ij/>) National Institutes of Health, Bethesda, MD (downloaded April 1, 2008).
- [38] Anwar A, Dehn D, Siegel D, Kepa JK, Tang LJ, Pietenpol JA, Ross D. Interaction of human NAD(P)H:quinone oxidoreductase 1 (NQO1) with the tumor suppressor protein p53 in cells and cell-free systems. *J Biol Chem* 2003;278:10368–73.
- [39] Sarg B, Koutzamani E, Helliger W, Rundquist I, Lindner HH. Postsynthetic trimethylation of histone H4 at lysine 20 in mammalian tissues is associated with aging. *J Biol Chem* 2002;277:39195–201.
- [40] Camporeale G, Zempleni J, Eissenberg JC. Susceptibility to heat stress and aberrant gene expression patterns in holocarboxylase synthetase-deficient *Drosophila melanogaster* are caused by decreased biotinylation of histones, not of carboxylases. *J Nutr* 2007;137:885–9.
- [41] Gralla M, Camporeale G, Zempleni J. Holocarboxylase synthetase regulates expression of biotin transporters by chromatin remodeling events at the SMVT locus. *J Nutr Biochem* 2008;19:400–8.
- [42] Manthey KC, Griffin JB, Zempleni J. Biotin supply affects expression of biotin transporters, biotinylation of carboxylases, and metabolism of interleukin-2 in Jurkat cells. *J Nutr* 2002;132:887–92.
- [43] Zempleni J, Mock DM. Uptake and metabolism of biotin by human peripheral blood mononuclear cells. *Am J Physiol Cell Physiol* 1998;275:C382–8.
- [44] SAS Institute (1999). StatView Reference SAS Publishing, StatView Reference, Cary, NC.
- [45] Cawthon RM. Telomere measurement by quantitative PCR. *Nucleic Acids Res* 2002;30:e47.
- [46] Simpson RT. Histones H3 and H4 interact with the ends of nucleosome DNA. *Proc Natl Acad Sci USA* 1976;73:4400–4.
- [47] Kristjuhan A, Svejstrup JQ. Evidence for distinct mechanisms facilitating transcript elongation through chromatin in vivo. *EMBO J* 2004;23:4243–52.
- [48] Lee CK, Shibata Y, Rao B, Strahl BD, Lieb JD. Evidence for nucleosome depletion at active regulatory regions genome-wide. *Nat Genet* 2004;36:900–5.
- [49] Erkina TY, Tschetter PA, Erkin AM. Different requirements of the SWI/SNF complex for robust nucleosome displacement at promoters of heat shock factor and Msn2- and Msn4-regulated heat shock genes. *Mol Cell Biol* 2008;28:1207–17.
- [50] Said HM. Recent advances in carrier-mediated intestinal absorption of water-soluble vitamins. *Annu Rev Physiol* 2004;66:419–46.
- [51] Camporeale G, Zempleni J. Biotin. In: Bowman BA, Russell RM, editors. Present knowledge in nutrition. Washington, DC: International Life Sciences Institute; 2006. p. 314–26.
- [52] Crisp SERH, Camporeale G, White BR, Toombs CF, Griffin JB, Said HM, Zempleni J. Biotin supply affects rates of cell proliferation, biotinylation of carboxylases and histones, and expression of the gene encoding the sodium-dependent multivitamin transporter in JAr choriocarcinoma cells. *Eur J Nutr* 2004;43:23–31.
- [53] Scheerger SB, Zempleni J. Expression of oncogenes depends on biotin in human small cell lung cancer cells NCI-H69. *Int J Vitam Nutr Res* 2003;73:461–7.
- [54] Freytag SO, Utter MF. Regulation of the synthesis and degradation of pyruvate carboxylase in 3T3-L1 cells. *J Biol Chem* 1983;258:6307–12.
- [55] Weinberg MD, Utter MF. Effect of thyroid hormone on the turnover of rat liver pyruvate carboxylase and pyruvate dehydrogenase. *J Biol Chem* 1979;254:9492–9.
- [56] Weinberg MD, Utter MF. Effect of streptozotocin-induced diabetes mellitus on the turnover of rat liver pyruvate carboxylase and pyruvate dehydrogenase. *Biochem J* 1980;188:601–8.
- [57] Majerus P, Kilburn E. Acetyl coenzyme A carboxylase. The roles of synthesis and degradation in regulation of enzyme levels in rat liver. *J Biol Chem* 1969;244:6254–62.
- [58] Nakanishi S, Numa S. Purification of rat liver acetyl coenzyme A carboxylase and immunochemical studies on its synthesis and degradation. *Eur J Biochem* 1970;16:161–73.
- [59] Commerford SL, Carsten AL, Cronkite EP. Histone turnover within nonproliferating cells. *Proc Natl Acad Sci USA* 1982;79:1163–5.
- [60] Djondjurov LP, Yancheva NY, Ivanova EC. Histones of terminally differentiated cells undergo continuous turnover. *Biochemistry* 1983;22:4095–102.
- [61] Podgornaya OI, Bugaeva EA, Voronin AP, Gilson E, Mitchell AR. Nuclear envelope associated protein that binds telomeric DNAs. *Mol Reprod Dev* 2000;57:16–25.
- [62] Ding X, Xu R, Yu J, Xu T, Zhuang Y, Han M. SUN1 is required for telomere attachment to nuclear envelope and gametogenesis in mice. *Dev Cell* 2007;12:863–72.
- [63] Schmitt J, Benavente R, Hodzic D, Hoog C, Stewart CL, Alsheimer M. Transmembrane protein Sun2 is involved in tethering mammalian meiotic telomeres to the nuclear envelope. *Proc Natl Acad Sci USA* 2007;104:7426–31.